

INFLUENCE OF DEFORMATION AND MOLYBDENUM CONTENT ON ACICULAR FERRITE FORMATION IN MEDIUM CARBON STEELS

C. Capdevila, J.P Ferrer, F.G. Caballero and C. García de Andrés

Department of Physical Metallurgy, Centro Nacional de Investigaciones Metalúrgicas (CENIM), Consejo Superior de Investigaciones Científicas (CSIC), Avda. Gregorio del Amo, 8, 28040 Madrid, Spain

ABSTRACT

The present work deals with the influence of deformation and molybdenum content on the subsequent austenite-to-acicular ferrite transformation during continuous cooling in medium carbon microalloyed steels. The results obtained demonstrate that higher deformation temperature induce a finer austenite grain size due to austenite recrystallisation processes during cooling down to austenite decomposition temperature. The finer austenite grain, the higher the molybdenum content and severity of deformation is. Likewise, it was concluded that molybdenum suppress pearlitic microstructure, and clearly delay proeutectoid ferrite field to longer times. By contrast, acicular ferrite transformation is enhanced in molybdenum rich steel, which not only affect the volume fraction but morphology of acicular ferrite also.

KEYWORDS

Forging steel, acicular ferrite, phase transformation, molybdenum, continuous cooling diagrams

INTRODUCTION

Acicular ferrite microstructure, which provides effective grain (structural) refinement, is one of the most desired microstructure that improves both strength and toughness. Recent experimental results [1-3] strongly indicate that a fine acicular ferrite microstructure can be obtained in medium carbon microalloyed forging steels. This subject represents a major and very exciting advance in the technology of steels. However, a deep understanding of the influences that the alloying elements have on the final microstructure should be reached to produce this kind of steels directly by industrial thermomechanical processes. Although the role of elements such as manganese has been thoroughly reported in literature [4-], the role of molybdenum, on the counterpart, is a subject that no so much attention on literature has been paid.

There is evidence to show that in many cases, acicular ferrite is in effect bainite, which nucleates intragranularly on inclusions. For example, the transformation of acicular ferrite occurs below the B_s temperature [6], the transformation exhibits an incomplete-reaction phenomenon [7], the growth of acicular ferrite causes a shape deformation which is characterised as an invariant plane strain with a large shear component, leading to a stored energy of about 400 J mol^{-1} , which is similar to that of bainite [8]. Like bainite, the acicular ferrite always has a well-defined crystallographic orientation relationship with the austenite grain in which it grows, and indeed, is restricted to grow in that grain because the coordinated motion of atoms cannot be sustained across an arbitrary grain boundary [7,8]. There is no partitioning of substitutional alloying elements [8]. Thus, it is expected that the transformation to acicular ferrite, as that of bainite, can be affected by elastic stress [9] and by the plastic deformation of austenite.

Therefore, the main aim of this work is two fold: Firstly, to clarify the role of the severe plastic deformation of austenite during forging process on the subsequent transformation of austenite – to – acicular ferrite, and secondly, to clarify the role of molybdenum on such transformation.

MATERIALS AND EXPERIMENTAL PROCEDURE

The chemical composition of the two forging steels studied is presented in Table 1. The material was supplied in the form of 50 mm square bars, obtained by conventional casting to an square ingot (2500 Kg weight) and hot rolling to bar. Cylindrical dilatometric test pieces of 2 mm diameter and 12 mm length were machined longitudinally to the rolling direction of the bar.

Table 1- Chemical composition (mass %)

	C	Mn	Si	Cr	Ni	Mo	V	Al	Ti	N(ppm)
Steel A	0.36	1.44	0.63	0.17	0.13	0.02	0.09	0.020	0.022	96
Steel B	0.38	1.44	0.62	0.07	0.04	0.16	0.10	0.026	0.016	122

An Adamel Lhomargy DT1000 high resolution dilatometer has been used to determine the CCT diagrams of this steel. The dimensional variations of the specimen are transmitted via an amorphous silica pushrod. These variations are measured by a LVDT sensor in a gas-tight enclosure enabling testing under vacuum or in an inert atmosphere. The temperature is measured with a 0.1 mm diameter Chromel-Alumel (Type K) thermocouple welded to the specimen. Cooling is carried out by blowing a jet of helium gas directly onto the specimen surface. The helium flow rate during cooling is controlled by a proportional servovalve. The excellent efficiency of heat transmission and the very low thermal inertia of the system ensure that the heating and cooling rates ranging from 0.003 K/s to approximately 200 K/s remain constant.

Thermomechanical cycles were simulated in a Bähr DIL 805A/D deformation dilatometer. To simplify the experiment, two of the three thermal parameters conditioning the state of austenitization were kept constant in the heating cycle: the heating rate, 10 °C/s, and the holding time, 180 s. Thus, the austenitization temperature is the only thermal parameter capable of modifying and predetermining the state of austenitization of this steel. Specimens were polished and etched in the usual way for metallographic examination. The microstructure was examined by light optical microscopy and PAGS was measured according to Underwood's intersection method [10].

RESULTS AND DISCUSSION

Effect of molybdenum on acicular ferrite microstructure

It is generally accepted that austenite decomposition is delayed in molybdenum containing steels leading to an increase in hardenability [5]. In the present work, the influence of molybdenum on the evolution of the austenite-to-acicular ferrite transformation as well as on the morphology of this phase has been investigated.

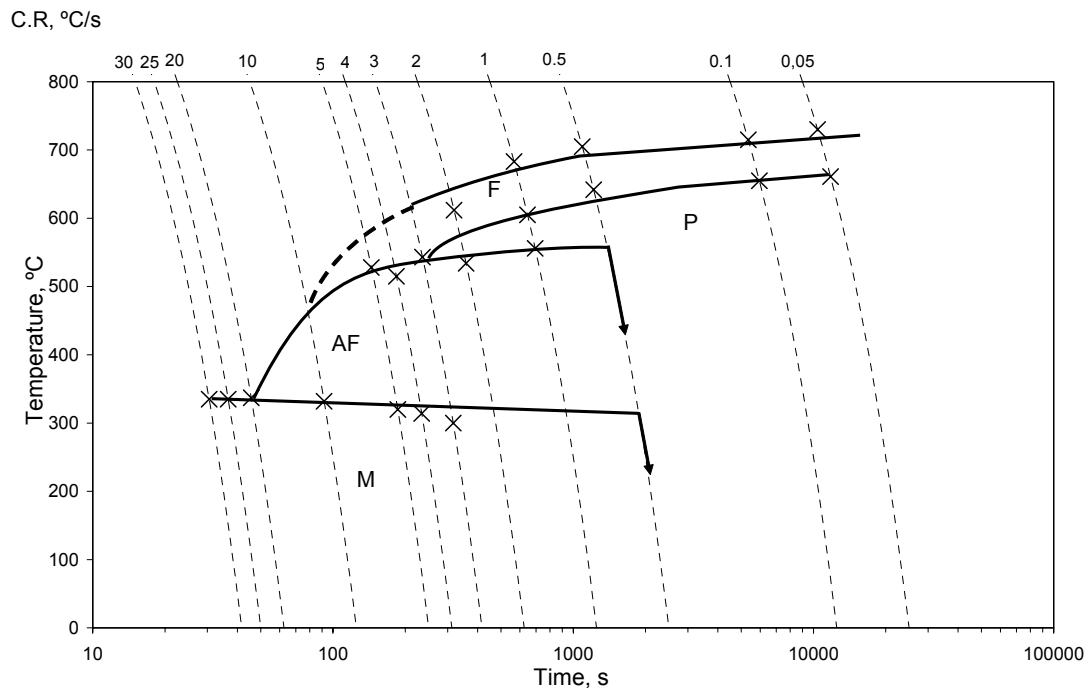


Figure 1. CCT diagram for the steel A, after an austenitization at 1250 °C. (F = Allotriomorphic Ferrite, P = Pearlite, AF = Acicular Ferrite M= Martensite).

The CCT diagrams of the two steels studied in this work are presented in Figures 1 and 2. Figure 1 shows that the non-isothermal austenite-to-acicular ferrite transformation in steel A occurs at cooling rates ranging from 25 Cs⁻¹ to 1 Cs⁻¹. The allotriomorphic ferrite formation is avoided cooling down at a rate higher than about 30 Cs⁻¹. Pearlite formation is suppressed if the cooling is carried out at a rate of 7 Cs⁻¹ or higher. The micrograph in Figure 3 (a) shows that, although pearlite formation is totally inhibited at a cooling rate of 10 °C s⁻¹, a fine layer of allotriomorphic ferrite which represents approximately the 7% of the microstructure covers the most part of the prior austenite grain boundaries. The intragranular formation of ferrite leads to a mainly acicular ferrite microstructure for steel A cooled at the above mentioned cooling rate. Nevertheless, the decomposition of austenite does not complete before the martensite start temperature is reached, which causes the apparition of a small amount of martensite at the later stages of the cooling. By contrast, at a cooling rate of 6 C s⁻¹ (Figure 3(b)), a reduction in the final amount of martensite is observed, the volume fraction of allotriomorphic ferrite increases to 10%, and a 2% of pearlite is also present in the final microstructure. At a cooling rate of 3 °C s⁻¹ (Figure 3(c)), significant amounts of allotriomorphic ferrite and pearlite are present in the final microstructure. Cooling rates lower than 2 °C s⁻¹ would promote the formation of a mixture of allotriomorphic ferrite and pearlite as the main microstructural components.

The formation of an allotriomorphic ferrite layer on the previous austenite grain boundaries is well known [11] to inhibit the formation of bainite and contributes indirectly to the nucleation of AF. However, the steel A presents a high tendency to form an AF microstructure instead of bainite, even in the absence of this ferrite layer. By cooling at a rate between 10 and 2 °C s⁻¹, the final microstructure is mainly AF. Fully acicular ferrite microstructures have also been obtained in this steel by isothermal treatments.

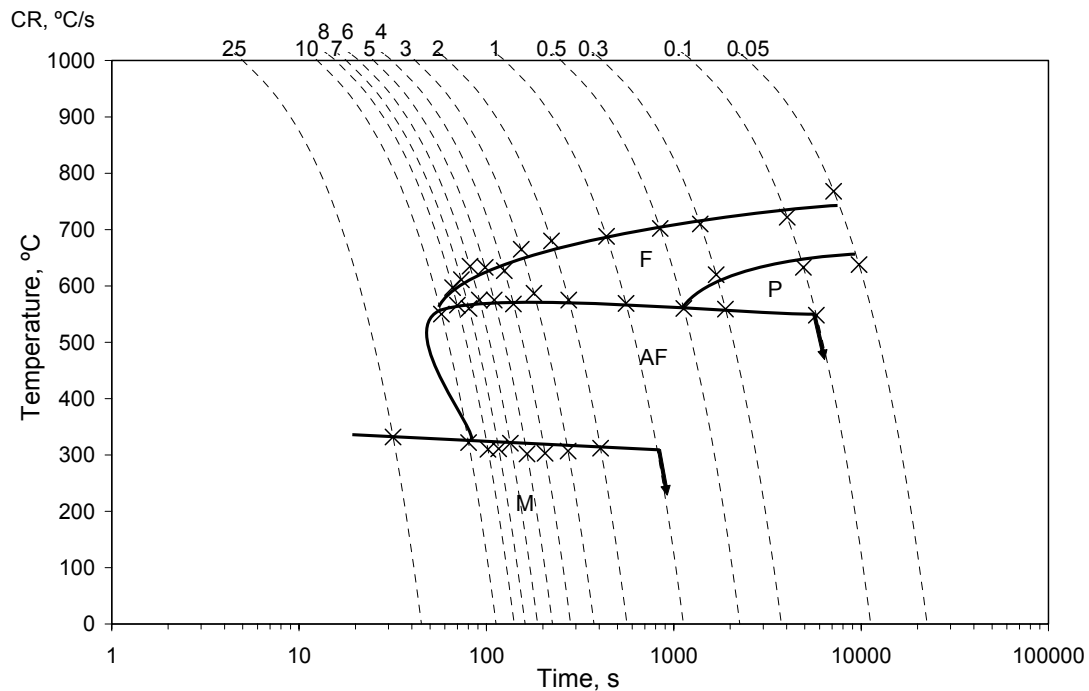


Figure 2. CCT diagram for the steel B, after an austenitization at 1125 °C. (F = Allotriomorphic Ferrite, P = Pearlite, AF = Acicular Ferrite M= Martensite)

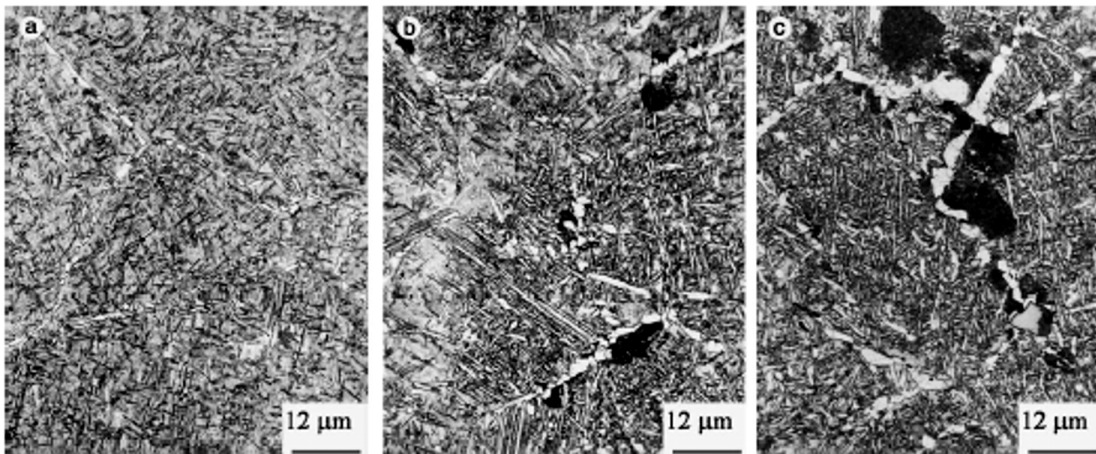


Figure 3. Microstructures obtained in steel A after the continuous cooling at (a) 10 °C^s⁻¹ (b) 6 °C^s⁻¹ and (c) 3 °C^s⁻¹.

The addition of Mo to the steel modifies the CCT curves. In comparison with the diagram for steel A in Figure 1, the pearlite region in the CCT diagram of steel B (Figure 2) is displaced to longer times. The region corresponding to the acicular ferrite transformation is expanded to lower cooling rates and slightly higher temperatures. It is observed that, like in steel A, the diminution of the allotriomorphic ferrite is not accompanied by the transition from acicular ferrite to bainite formation. As a result, the range of cooling rates leading to the formation of acicular ferrite as the predominant microstructural constituent in the Mo containing steel ranges now from 6 °C^s⁻¹ to 0.3 °C^s⁻¹. The produced microstructures for different cooling rates are shown in Figure 4. The differences between steels A and B can be understood comparing the micrographs in Figures 3 and 4. It can be seen that a 10% of allotriomorphic ferrite is found in steel A upon cooling at 6 °C^s⁻¹ but it is not distinguishable in steel B even at a much lower cooling rate of 0.75 °C s⁻¹. On the other hand, cooling rates higher than 6 °C^s⁻¹ applied to steel B produce significant amounts of martensite. According to the CCT diagrams in Figures 1 and 2, Mo does not seem to have a large effect on the

M_s martensite start temperature on quenching. However, when acicular ferrite forms, the presence of Mo in the steel enhances the apparition of martensite in the final microstructure, even for cooling rates as low as $0.6\text{ }^\circ\text{C s}^{-1}$. This is probably due to the influence this element has on the transformation kinetics and on the hardenability. In the absence of this element in the steel, martensite formation requires cooling rates higher than $3\text{ }^\circ\text{C s}^{-1}$.

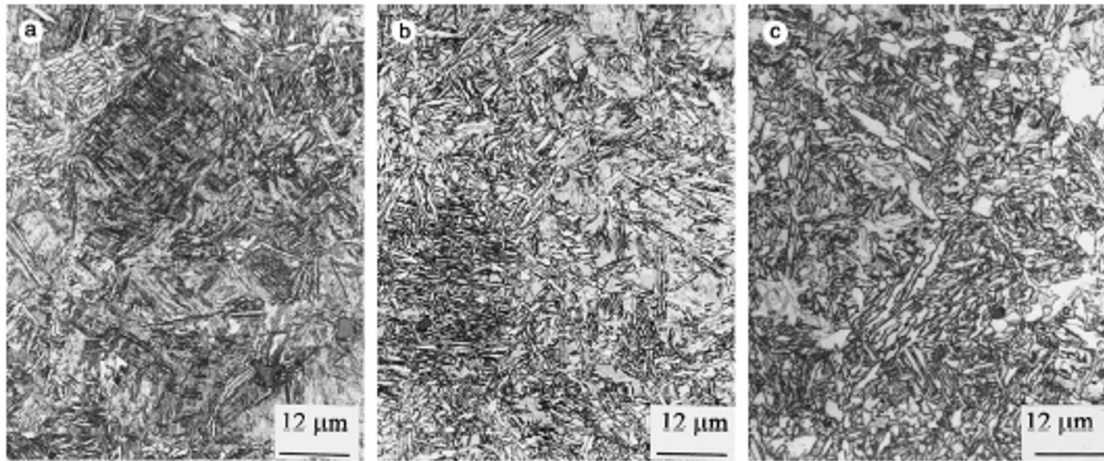


Figure 4. Microstructures obtained in steel B after continuous cooling at a) $6\text{ }^\circ\text{C s}^{-1}$, b) $3\text{ }^\circ\text{C s}^{-1}$ and c) $0.75\text{ }^\circ\text{C s}^{-1}$.

Isothermal treatments have been carried out to investigate comparatively the behavior of both steels and the effect of the Mo on the acicular ferrite microstructure. The microstructural compositions obtained with the isothermal treatments carried out at temperatures in the range $500\text{--}400\text{ }^\circ\text{C}$ are shown in Table 2 for both steels. It can be seen that, for temperatures lower than about $450\text{ }^\circ\text{C}$, the microstructure is mainly acicular ferrite. Above this temperature, different mixtures of ferrite, pearlite and acicular ferrite form. The final microstructures obtained for a holding time of 20 min at $450\text{ }^\circ\text{C}$ are shown in Figure 5 for both steels. It can clearly be seen in the micrographs that Mo not only affects the transformation kinetics, as seen before, but also modifies the morphology of the transformation product. Steel A exhibits a microstructure after this treatment formed by the well known randomly oriented ferrite plates while steel B develops packets formed by different parallel sub-units. This type of microstructure can be erroneously interpreted as being bainite if the evolution of the transformation is not carefully followed from the early stages. At this stage, sites where nucleation takes place makes the difference between bainite and acicular ferrite. Looking at the partially transformed microstructures produced by interrupted isothermal tests, see Figure 6, it can be seen that primary acicular ferrite plates in steel A nucleate on the second phase particles. These have been identified as being MnS particles covered by a shell of CuS. This shell seems to be favorable in terms of acicular ferrite formation, as discussed by Madariaga and Guitierrez [12]. The same type of particles also produces AF nucleation in steel B [13]. It has been shown that the transformation can progress in two different ways through the autocatalytic nucleation of new plates in different orientations to the primary ones or by the formation of subunits parallel to them [14]. In the first case, the result is the typical interlocking microstructure of acicular ferrite that can be seen in Figure 5(a) for the steel A at $450\text{ }^\circ\text{C}$. Steel B behaves according to the second type of morphology.

This transition between both types of transformation relates to the carbon mobility which is expected in turn to depend not only on the treatment temperature but also on the steel composition. As can be seen in Figure 6(c), the Mo containing steel presents an evolution of the transformation at $450\text{ }^\circ\text{C}$ similar to that exhibited by the steel A at $400\text{ }^\circ\text{C}$. The same type of SEM and TEM analysis carried out previously [14] is now under progress for Mo containing steel. However, according to

the present results, it seems that the addition of Mo has raised the temperature of transition between upper and lower acicular ferrite and consequently the temperature of formation of sheaves instead of plates.

Table 2. Constituents of the final microstructures after isothermal heat treatments.

Temperature (°C)	Microstructure	
	Steel A	Steel B
500	P, AF, F	AF (SPP), P
450	AF	AF (SPP)
400	AF (SPP)	AF (SPP)

AF = Acicular Ferrite, AF (SPP) = Acicular Ferrite with Sheaves of Parallel Plates, P = Pearlite, F = Allotriomorphic Ferrite.

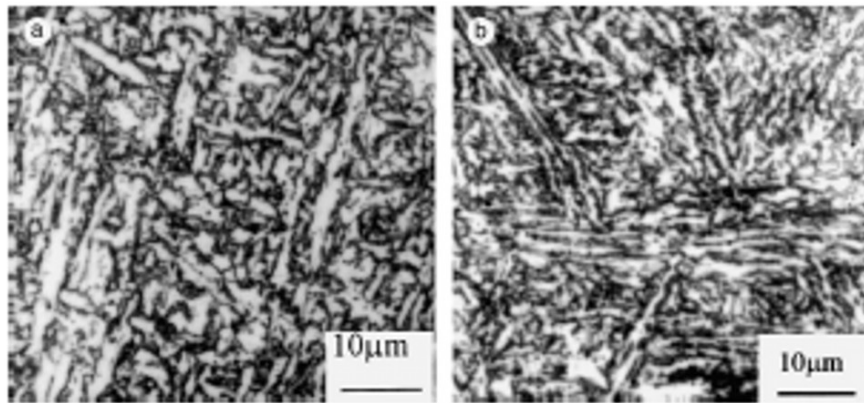


Figure 5. Final microstructures obtained by isothermal treatment during 20 min at 450 °C a) steel A and b) steel B.

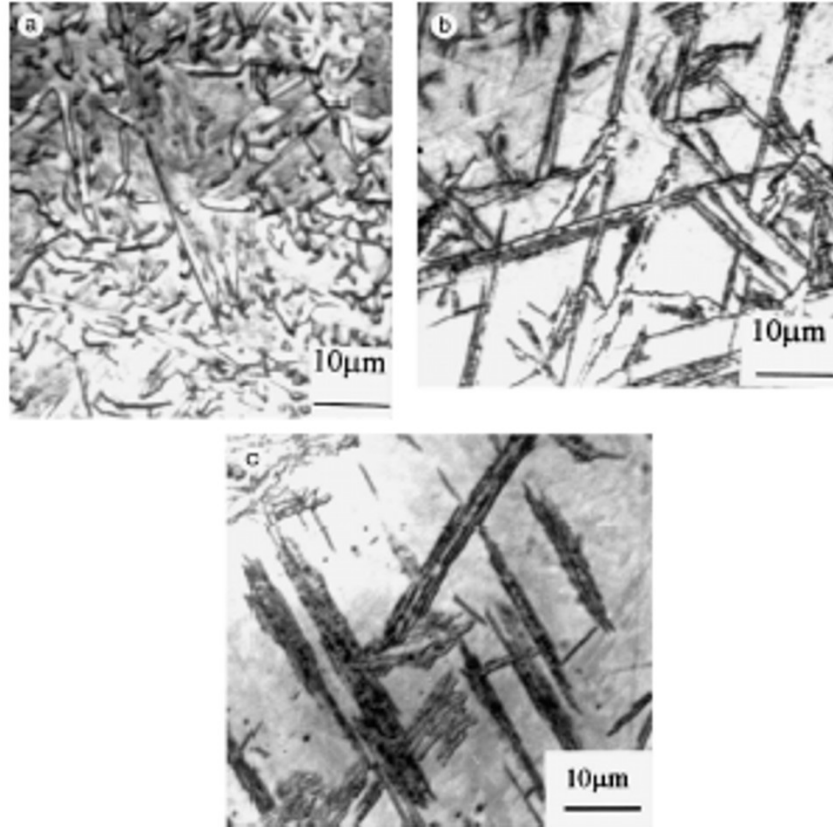


Figure 6. Optical micrographs a) steel A held during 10s at 450°C, b) steel A held during 20s at 400 °C and c) steel B held during 20s at 450 °C followed in all the cases by water quenching.

Effect of forging temperature on acicular ferrite transformation

The effect of forging temperature was studied by means of thermomechanical cycles as the ones presented in Figure 7. Since dynamic recrystallization is expected during deformation, and in order to avoid very coarse grain sizes, rapid cooling is performed from deformation to 1000 °C. Hence, continuous cooling to room temperature was performed.

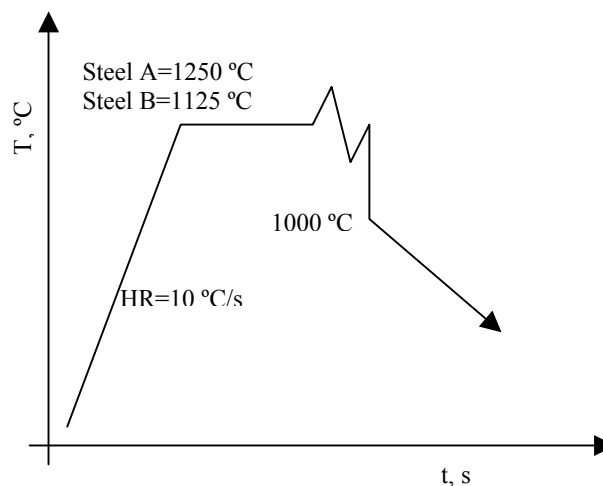


Figure 7. Scheme of thermomechanical cycle applied

In order to avoid the effect of previous austenite grain size (PAGS), the same PAGS in both steels has been considered. In this sense, a value of $63 \pm 7 \mu\text{m}$ was measured after holding at 1250 °C for

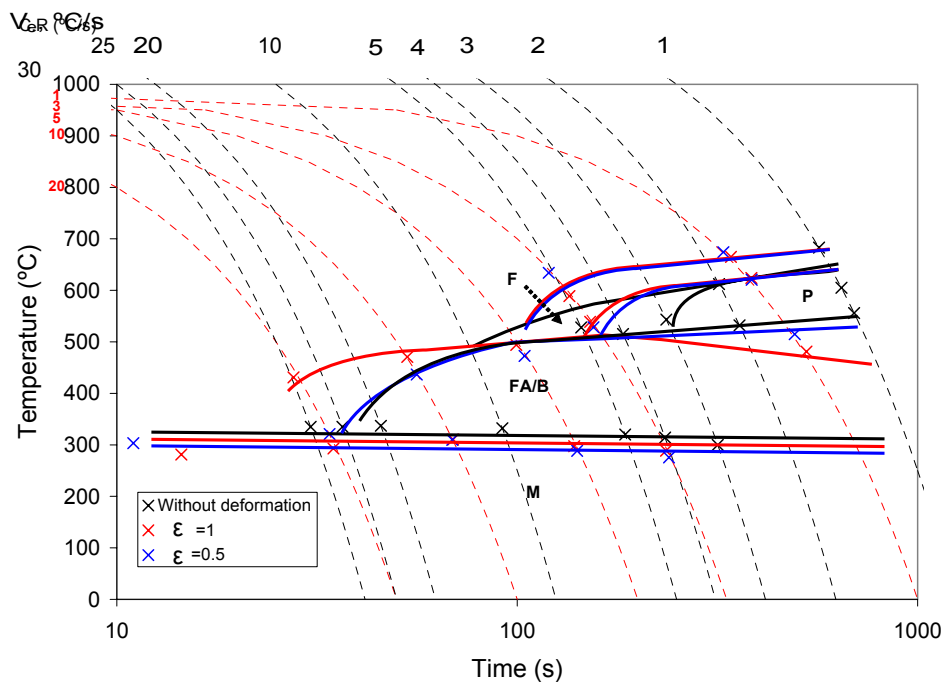
180 s in steel A, and a value of $66 \pm 7 \mu\text{m}$ was obtained after holding at 1125 °C for 180 s in steel B, respectively. Deformation conditions are listed in Table 3.

Table 3. Deformation parameters

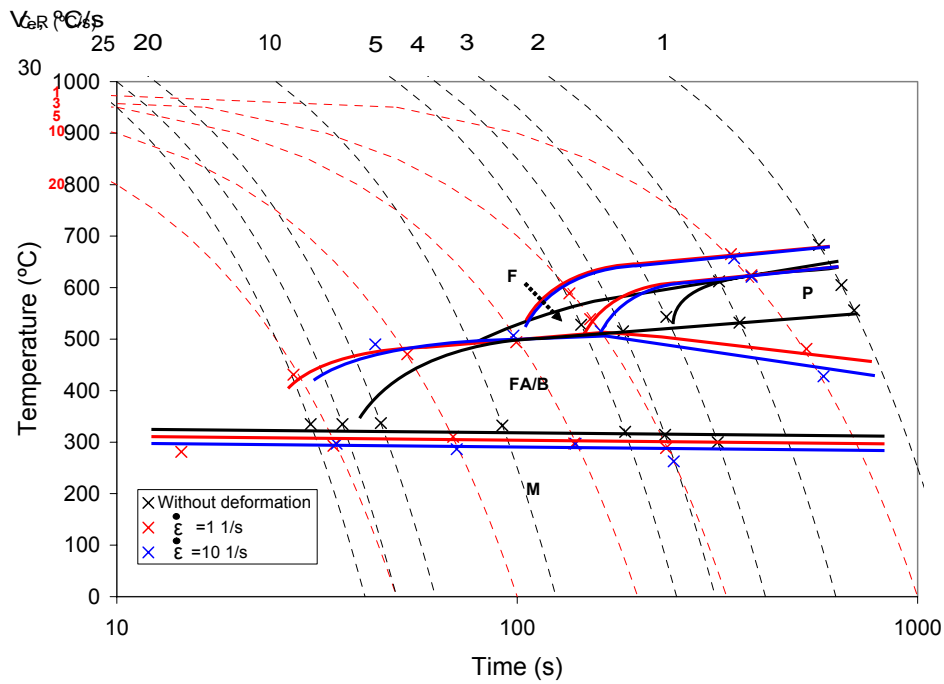
Material	ε	$\dot{\varepsilon}$ (s ⁻¹)	T (°C)	RAGS (μm)
Steel A_1	0.5	1	1250	48 ± 7
Steel A_2	1	1	1250	41 ± 6
Steel A_3	1	10	1250	38 ± 2
Steel B_1	1	10	1125	17 ± 2

The values of recrystallized grain sizes (RAGS) are listed in Table 3. It is clear from the data that considerably grain refinement is obtained after deformation. Likewise, since deformation temperature for steel B is smaller, the combined effect of higher nucleation of recrystallized austenite grains in the deformed matrix, together with a slow grain growth process after recrystallization, can explain the finer grain size obtained.

Figures 8 and 9 show a comparison between the CCT diagrams in both steels with and without deformation. It is clear that hardenability is decreased in both steel under all deformation conditions. In this sense, pro-eutectoid phases and pearlite are enhanced. Likewise, acicular ferrite is also enhanced in detriment of martensite. This is especially significant in Mo – rich steel (Figure 10).



(a)



(b)

Figure 8. Effect of (a) deformation and (b) deformation rate on CCT diagrams for steel A.

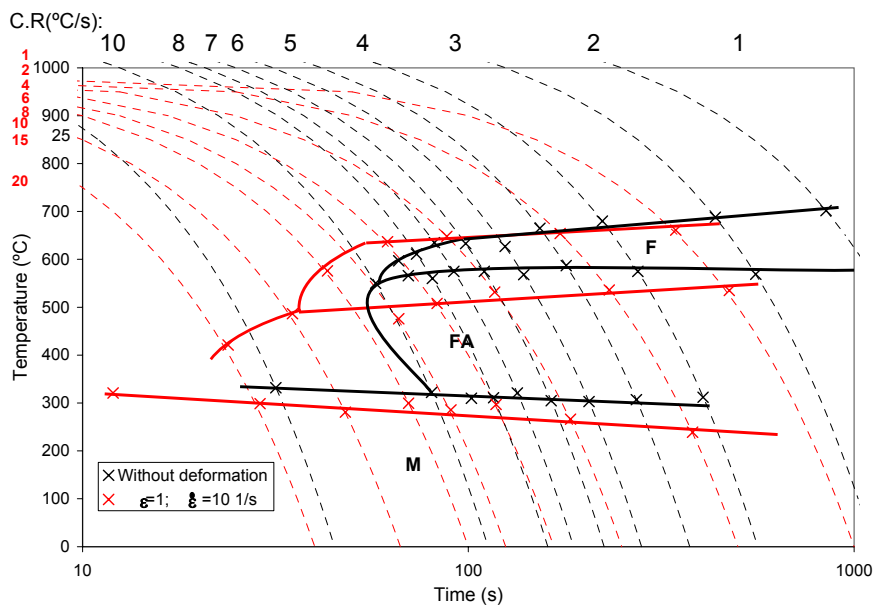


Figure 9. Effect of deformation on CCT diagram for steel B

The separate effect of deformation and deformation rate has been analysed in steel A. As degree of deformation at high temperature increases, a refinement of austenite grain is induced, and hence, hardenability is reduced. Therefore, allotriomorphic ferrite and pearlite are prone to be formed consuming most of the austenite volume before acicular ferrite transformation could take place. In this sense, it could be concluded that deformation at high temperature decrease the amount of acicular ferrite obtained in the microstructure comparing the same thermal cycle (Figure 11). On the other hand, it is also worth noting that deformation rate does not affect significantly the transformation fronts in steel A, which is consistent with the idea that fully recrystallization of austenite takes place before austenite decomposition starts.

Concerning steel B, it is clear that deformation at high temperature shifts the transformation fronts to smaller times because the lower hardenability caused by the decrease on austenite grain size after deformation. However, as it was observed above, Mo content increases hardenability so badly that the decrease produced by the deformation at high temperatures compensate such effect. In this sense, meanwhile cooling an undeformed austenite at rates between 6 and 0.7 °C/s in steel B produce acicular ferrite as the major component, such window is shifted to cooling rates ranging from 10 to 4 °C/s in deformed steel. Thus, acicular ferrite is enhanced in this steel as compare with undeformed steel.

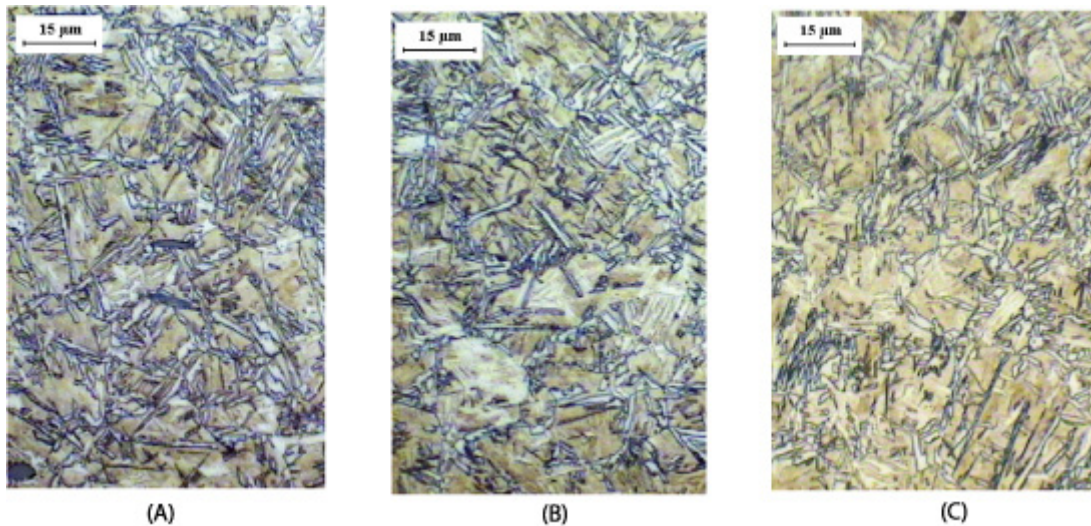


Figure 10. Micrographs of deformed Steel B and cooled at (a) 6, (b) 8, and (c) 10 °C/s.

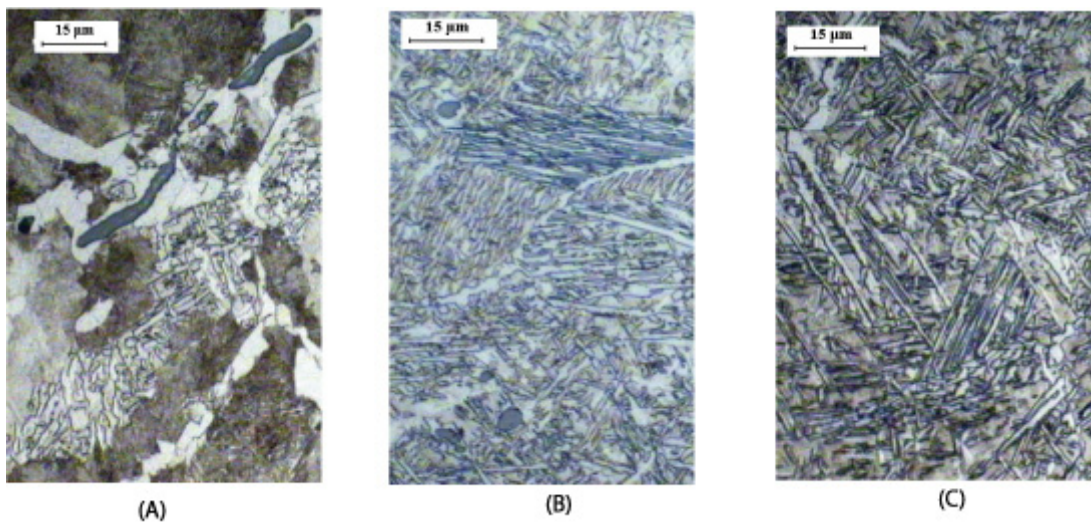


Figure 11. Micrographs of deformed Steel A ($\epsilon=1$ and $\dot{\epsilon}=1$), and cooled at (a) 1, (b) 3, and (c) 5 °C/s.

CONCLUSIONS

- 1- Molybdenum not only affects the transformation kinetics but also modifies the morphology of the acicular ferrite.

- 2- Molybdenum favors the acicular ferrite formation but increases the amount of martensite being present in the final microstructure. In Mo containing steel, the formation of this phase is the main variable limiting the design of useful cooling cycles in order to get microstructures with enhanced mechanical properties.
- 3- Because of dynamic recrystallisation, the austenite grain size after forging is sensibly lower than that without deformation. The finer grain size, the higher Mo content and deformation level.
- 4- Since finer austenite grain size after recrystallisation is obtained during forging, the hardenability decreases, increasing the amount of allotriomorphic ferrite and pearlite. The AF front is also enhanced in detriment of martensite, specially on Mo – rich steel.

REFERENCES

1. C. GARCIA DE ANDRES, C. CAPDEVILA, I. MADARIAGA and I. GUTIERREZ, *Scripta Materialia* **45**, (2001) p.709.
2. C. GARCÍA DE ANDRÉS, C. CAPDEVILA, F.G. CABALLERO and D. SAN MARTÍN, *J. Mat. Sci.* **36**, (2001), p.565.
3. C. GARCÍA DE ANDRÉS, C. CAPDEVILA and F.G. CABALLERO, in *Proc.of European Conference on Materials in Oceanic Environment. EUROMAT'98. Vol. II. Ed. L. Faria, Lisboa, (1998), p.217.*
4. K.R. KINSMAN and H.I. AARONSON, *Transformation and hardenability in steels*, Climax Molybdenum co, Ann Arbor, Michigan, (1967), p.39
5. H.W. PAXTON and E.C. BAIN, *Alloying elements in steels*, ASM, Metals Park, OH, 1966:274.
6. S.S. BABU and H.K.D.H. BHADSHIA, *Mater. Sci. Tech.* **6**, (1990), p.1005.
7. H.K.D.H. BHADSHIA and J.W. CHRISTIAN, *Metall. Trans. A* **21**, (1990), p.767.
8. M. STRANGWOOD, Ph.D. Thesis, University of Cambridge, UK, 1987.
9. S.S. BABU and H.K.D.H. BHADSHIA, *Mater. Sci. Eng. A* **156**, (1992), p. 1.
10. G.F. VANDER VOORT, in *'Metallography. Principles and Practice'*, 427-444, 1984, New York, McGraw-Hill Book Company.
11. R.A. RICKS, P.R. HOWELL and G.S. BARRITE, *J. Mater. Sci.* **17**, (1982), p.732.
12. I. MADARIAGA and I. GUTIERREZ, *Acta Mater.* **47**, (1999), p.951.
13. I. MADARIAGA, PhD thesis, Univ. Navarra, San Sebastian, Spain, 1999.
14. M. DIAZ-FUENTES, I. MADARIAGA and I. GUTIERREZ, in *Proc. of J.J. Jonas Symposium on Thermomechanical Processing of steels - COM'2000, Met. Soc., Canada, (2000), p.489.*